

A new high-throughput screening instrument for libraries of combinatorial heterogeneous catalysts is presented on the following pages. This instrument can measure the activity *and* selectivity of a single catalyst within one minute.

High-Throughput Synthesis and Screening of Combinatorial Heterogeneous Catalyst Libraries

Peijun Cong, Robert D. Doolen, Qun Fan, Daniel M. Giaquinta, Shenheng Guan, Eric W. McFarland, Damodara M. Poojary, Kyle Self, Howard W. Turner, and W. Henry Weinberg*

Combinatorial chemistry has had an enormous impact on drug discovery research in the pharmaceutical and biotechnology industries in recent years. It is now being extended to the discovery of new solid-state materials.^[1–6] Heterogeneous catalysts is one class of solid-state inorganic materials that is an obvious and attractive area for combinatorial exploration. Heterogeneous catalysts are at the core of modern chemical and petroleum industries, and they are discovered and optimized through lengthy and largely trial-and-error procedures. Combinatorial synthetic techniques offer the means to synthesize rapidly a large number of chemically distinct entities. The discovery process for new heterogeneous catalysts can be shortened dramatically if their catalytic properties can be measured in a similarly high throughput fashion. There have been some reports pertaining to the issue of high-throughput screening of heterogeneous catalyst libraries.^[7–9] The techniques are based either on infrared thermography^[7, 9] or resonance-enhanced multiphoton ionization.^[8] Although infrared thermography can identify exothermic reactions, there is no chemically specific information, which renders the technique of limited general value. Senkan^[8] recently applied resonance-enhanced multiphoton ionization detection to the screening of an eight-member catalyst library for the dehydrogenation of cyclohexane to benzene. Since only the benzene product was measured, however, no selectivity information was available.

A systematic and integrated approach is necessary to realize fully the promise of combinatorial chemistry in heterogeneous catalysis. We report here preliminary results in developing such an approach through the catalytic oxidation of CO and the reduction of NO by metal alloy catalysts that consist of Rh, Pd, Pt, and Cu as an example. The oxidation of CO by either O₂ or NO is one of most thoroughly studied heterogeneous catalytic reactions^[10–12] and is thus an ideal system to test and validate the combinatorial synthesis and screening techniques.

A 15 × 15 × 15 triangular library that contained 120 different catalysts was prepared by depositing three metals (for example, Rh, Pd, and Pt) by radiofrequency (RF) sputtering through masks onto a quartz wafer (75 mm diameter, 1.5 mm thick); each catalyst has a diameter of 1.5 mm and a thickness of approximately 100 nm. Each site at the apex of the triangle contains the pure metal, with its concentration decreasing linearly when going away from the apex and reaching zero at

the adjacent side of the triangle; the adjacent side is composed of binary mixtures of the other two metals. A row of 16 blank elements was added to one side of the triangle as a control to provide a measure of the background of the system. The deposition was accomplished by ten repeated steps. A total of 10 nm of material per catalyst site, with the desired concentration of each metal, was deposited in each step. The total deposition time for such a library is about one hour. The superlattice structure of the films is important for the mixing of the three metals. Powder X-ray data^[13] taken after the library was annealed at 773 K in a stream of 5 % H₂ and 95 % Ar for two hours show no diffraction signals that originate from the pure metals in the mixtures, which indicates good intermetal mixing in the various alloy catalysts. Given the density of the noble metals (10–20 g cm^{−3}) and the diameter (1.5 mm) and thickness (100 nm) of the catalyst, the loading per site is approximately 2–4 μg. The Rh-Pt-Cu and Rh-Pd-Cu libraries were prepared in a similar manner. An additional Rh-Pd-Pt library was made by sol–gel based techniques by using automated liquid deposition robotics. The results are identical to those obtained from RF-sputtered libraries.

A schematic representation of the experimental apparatus for screening catalytic activity is shown in Figure 1. The substrate containing the catalyst library is loaded onto a two-dimensional screening stage underneath a probe with concentric tubings for gas delivery/removal and sampling.^[14] Only

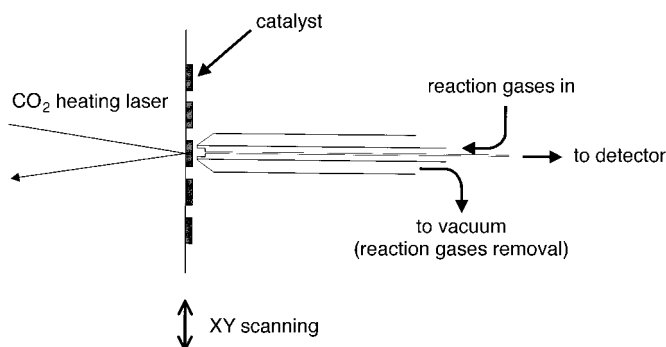


Figure 1. Schematic representation of the experimental apparatus used for screening catalytic activity. For more details see the text and ref. [14].

the catalyst that is being tested is exposed to the reactant stream, and the excess reactants are removed from the system by a vacuum line. The catalyst is heated by a CO₂ laser to the desired temperature before the measurement commences. No other catalyst experiences heat or the reactant stream since the heating is localized and the reactants are delivered locally, which allows a measurement of the initial activity (and selectivity) of each catalyst. The measurement of product as well as reactant concentrations is achieved by sampling the gas mixture directly above the catalyst and transporting it into a mass spectrometer or an optical detector through a capillary transfer line. Each measurement takes about one minute to complete, and only slightly more than two hours are needed to complete the 136 element library. To accomplish a similar goal with individually loaded micro-reactors would take hundreds, if not thousands, of hours.

[*] W. H. Weinberg, P. Cong, R. D. Doolen, Q. Fan, D. M. Giaquinta, S. Guan, E. W. McFarland, D. M. Poojary, K. Self, H. W. Turner
Symyx Technologies
3100 Central Expressway, Santa Clara, CA 95051 (USA)
Fax: (+1) 408-748-0175
E-mail: hweinberg@symyx.com

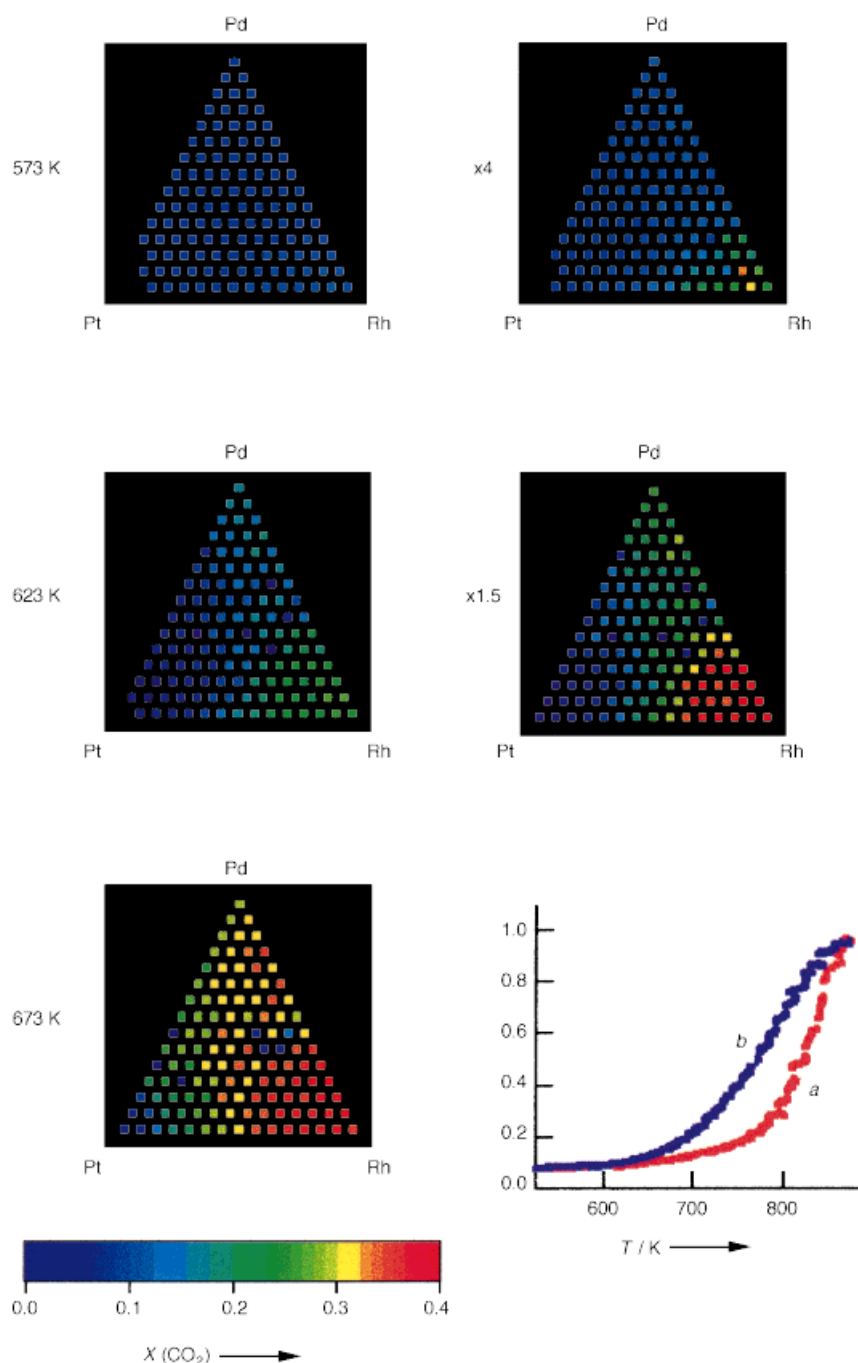


Figure 2. CO_2 production from a Rh-Pd-Pt ternary library. The displayed ion current (in 10^{-10} A) was corrected for filament emission current drift in the ion source. For clarity the data at 573 K and 623 K were rescaled and replotted in the right panel. See the text for details. The hysteresis loop of one of the elements in the library, pure Pt, is displayed in the lower right corner. The ordinate shows the ion current of CO_2 produced, in units of 10^{-10} A. The heating (a) and cooling (b) rates are both 1 K s^{-1} .

Figure 2 shows the CO_2 production from the Rh-Pd-Pt library at three different temperatures. The reaction was carried out with a mixture of CO, O_2 , and Ar in a ratio of approximately 2:1:4 and a pressure of about one atmosphere. Clearly, the order of activity for producing CO_2 at all three temperatures is $\text{Rh} > \text{Pd} > \text{Pt}$. This is in good agreement with results from experiments with single-crystalline surfaces as well as supported catalysts.^[11, 12, 15] The oxidation of CO proceeds in two distinct regimes on the platinum group

metals. At temperatures below the ignition point the reaction is relatively slow and is limited by the desorption of CO. When the surfaces reach the ignition temperature a kinetic phase transition that involves CO desorption occurs. Above this temperature the reaction proceeds much faster. These two regimes have different apparent activation energies and kinetic orders in CO and O_2 . There may also be hysteresis behavior, that is, the reaction rate may have two values at the same temperature depending on whether the catalyst is being heated or cooled. The hysteresis curve for pure Pt is shown in the lower right corner of Figure 2.

Some of the discontinuities in catalyst activity seen in Figure 2 (namely, low activity elements surrounded by much more active elements) may be caused by these kinetic instabilities. They are not likely to be caused by thermal damage, since different catalysts show low activities in different runs. In spite of these discontinuities, the global trend across the ternary system is obvious and reproducible. The more active elements are localized in the Rh-rich region, and the most active element below 623 K has the composition of 86 % Rh, 7 % Pd, and 7 % Pt. At 673 K the peak of activity shifted one to two gradient steps further away from the Rh corner and contains 79–71 % Rh. The reaction rate is not a sensitive function of the remaining Pt to Pd ratio. The enhancement of the most active catalyst relative to pure Rh is between 10 and 30 %, depending on the reaction temperature.

While it is interesting to observe the small, yet significant, enhancement of catalytic activity that arises from metal alloying, it does not constitute a major breakthrough in finding a superior oxidation catalyst for CO. On the other hand, if one of

the expensive noble metals could be replaced by a much less expensive metal and the resulting catalyst still maintain significant oxidation activity the situation might be different. To explore such a possibility Cu was introduced as a replacement for one of the noble metals. Figure 3 shows the results from a Rh-Pd-Cu library. This library was made in the same way as the Rh-Pd-Pt one, except that the total thickness of the film was 800 \AA rather than 1000 \AA (eight deposition steps instead of ten).

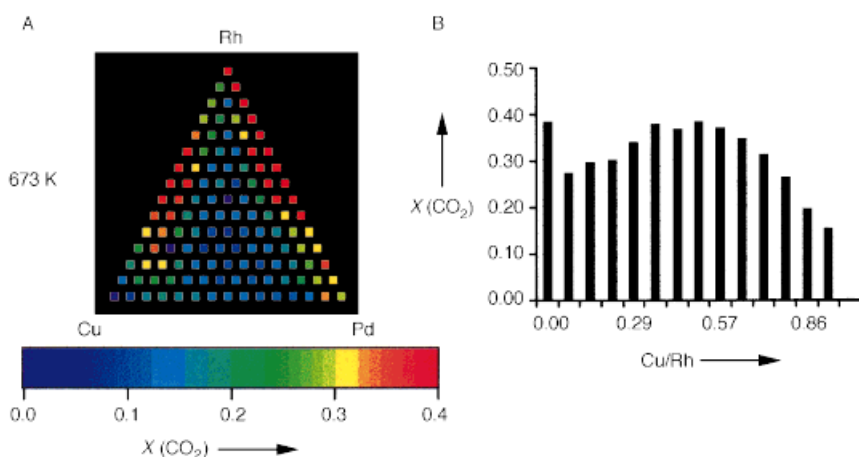


Figure 3. A) CO_2 production as measured by ion current (in units of 10^{-10} A) from a Rh-Pd-Cu ternary library at 673 K. B) The same data along the Rh-Cu binary axis replotted. The abscissa shows the mole fraction of Cu.

The performance of Rh-Cu binary mixtures is worth particular attention (see Figure 3). The 1:1 Cu:Rh catalyst is as active as the pure Rh catalyst at 673 K. While the activity of pure Cu is at least two orders of magnitude lower than that of Rh, a mixture of 93 % Cu and 7 % Rh maintains 40 % of the activity of pure Rh, and this trend is also observed at lower temperatures. Furthermore, Pt-Cu and Pd-Cu binaries show similar enhancements over the respective pure metals, and the enhancement is stronger at low temperatures than at high temperatures. The maxima are located on the Cu-rich side of the binaries at an approximately 60:40 ratio of Cu:Pt(Pd). These findings are in general agreement with recent literature on Cu modified (through evaporative coating) single-crystalline surfaces of Rh,^[16] Pt,^[17] and Pd.^[18] A preliminary aging test was performed on the 1:1 Rh:Cu alloy by observing the activity for more than 60 minutes at one atmosphere and 673 K. A 30 % reduction in activity was observed, which is less than that reported by Szanyi and Goodman^[16] for a Rh(100) surface with Cu overlayers.

The oxidation of CO by NO ($\text{CO} + \text{NO} \rightarrow \text{CO}_2 + \frac{1}{2}\text{N}_2$) is a more complex and challenging reaction relative to the oxidation of CO by O_2 . The reaction probabilities are much smaller,^[15] and incomplete reduction of NO to N_2O is possible. To distinguish the N_2 that is produced from unreacted CO and to distinguish N_2O from CO_2 in the mass spectrometer, ^{15}NO was employed. The same Rh-Pd-Pt library used for the oxidation of CO by O_2 reaction was used also for the oxidation with NO after regeneration in 5 % H_2 in Ar at 500 °C for two hours. The results are summarized in Figure 4. The reactions were carried out at 673, 773, and 873 K because of the lower reaction probabilities. The reactant mixture of CO, NO, and Ar was delivered with a 1:1:6 ratio at approximately one atmosphere. The order of activity for N_2 and CO_2 (not shown) production is once again Rh > Pd > Pt. This trend is also well documented in the literature^[15, 19, 20]. In general, the Rh-Pt binaries are more active than Rh-Pd alloys. The N_2O production, however, exhibits a quite interesting trend. At 673 K Rh and Rh-Pt alloys produced the most N_2O ; at 773 K this maximum shifted to Rh-Pd alloys; and at 873 K this reaction became less competitive

relative to the complete reduction of NO to N_2 , and the maximum activity shifted to the Pd-rich region along the Pd-Rh binary axis. The following trends are observed when the selectivity of the individual catalysts at fixed temperatures is considered. The ratio of N_2 to N_2O for Rh at 673 K is 1.2:1, after the ion currents are corrected for ionization efficiencies; this ratio is 22:1 at 873 K. The same ratio changed from 2.5:1 to 1.5:1 for Pd. Clearly, the N_2 production channel is favored at high temperatures for Rh and Rh-rich catalysts. On the other hand, the N_2O channel becomes relatively more important at high temperatures for Pd and Pd-rich catalysts. This finding correlates well with the branching ratios of

the same reaction on single-crystalline Pd surfaces reported by Vesecky et al.^[21]

Rapid catalyst deactivation was observed when libraries of Cu were screened for the oxidation of CO by NO. The Rh-Cu binaries showed significant enhancement in catalytic activity over pure Rh for both N_2 and N_2O production immediately after they had been annealed under a reducing atmosphere. However, this enhancement decays to less than that of Rh within a few minutes of exposure to the reactants at 673 K or higher. After this short “aging” time, the catalytic activity along the Rh-Cu axis can be described as an approximately linear decay from Rh to Cu, with Cu being no different from a blank element.

In summary, integrated combinatorial synthesis and screening methodologies have been developed for heterogeneous catalysis. This approach was demonstrated with the $\text{CO} + \text{O}_2$ and $\text{CO} + \text{NO}$ reactions with noble metal as well as Cu substituted noble metal libraries. The trends observed for the noble metal libraries are in complete agreement with the more limited data set reported previously in the literature. For the Cu-containing libraries, the Rh-Cu binary mixtures showed promising oxidation activity.

Received: October 19, 1998 [Z12542IE]
German version: *Angew. Chem.* **1999**, *111*, 508–512

Keywords: combinatorial chemistry • heterogeneous catalysis • mass spectrometry • screening methods

- [1] X.-D. Xiang, X. Sun, G. Briceno, Y. Lou, K.-A. Wang, H. Chang, W. G. Wallace-Freedman, S.-W. Chen, P. G. Schultz, *Science* **1995**, *268*, 1738–1740.
- [2] G. Briceno, H. Chang, X.-D. Sun, P. G. Schultz, X.-D. Xiang, *Science* **1995**, *270*, 273–275.
- [3] X.-D. Sun, K.-A. Wang, Y. Yoo, W. G. Wallace-Freedman, C. Gao, X.-D. Xiang, P. G. Schultz, *Adv. Mater.* **1997**, *9*, 1046–1049.
- [4] J. Wang, Y. Young, C. Gao, I. Takeuchi, X. Sun, H. Chang, X.-D. Xiang, P. G. Schultz, *Science* **1998**, *279*, 1712–1714.
- [5] E. Danielson, J. H. Golden, E. W. McFarland, C. M. Reaves, W. H. Weinberg, X. D. Wu, *Nature* **1997**, *389*, 944–948.

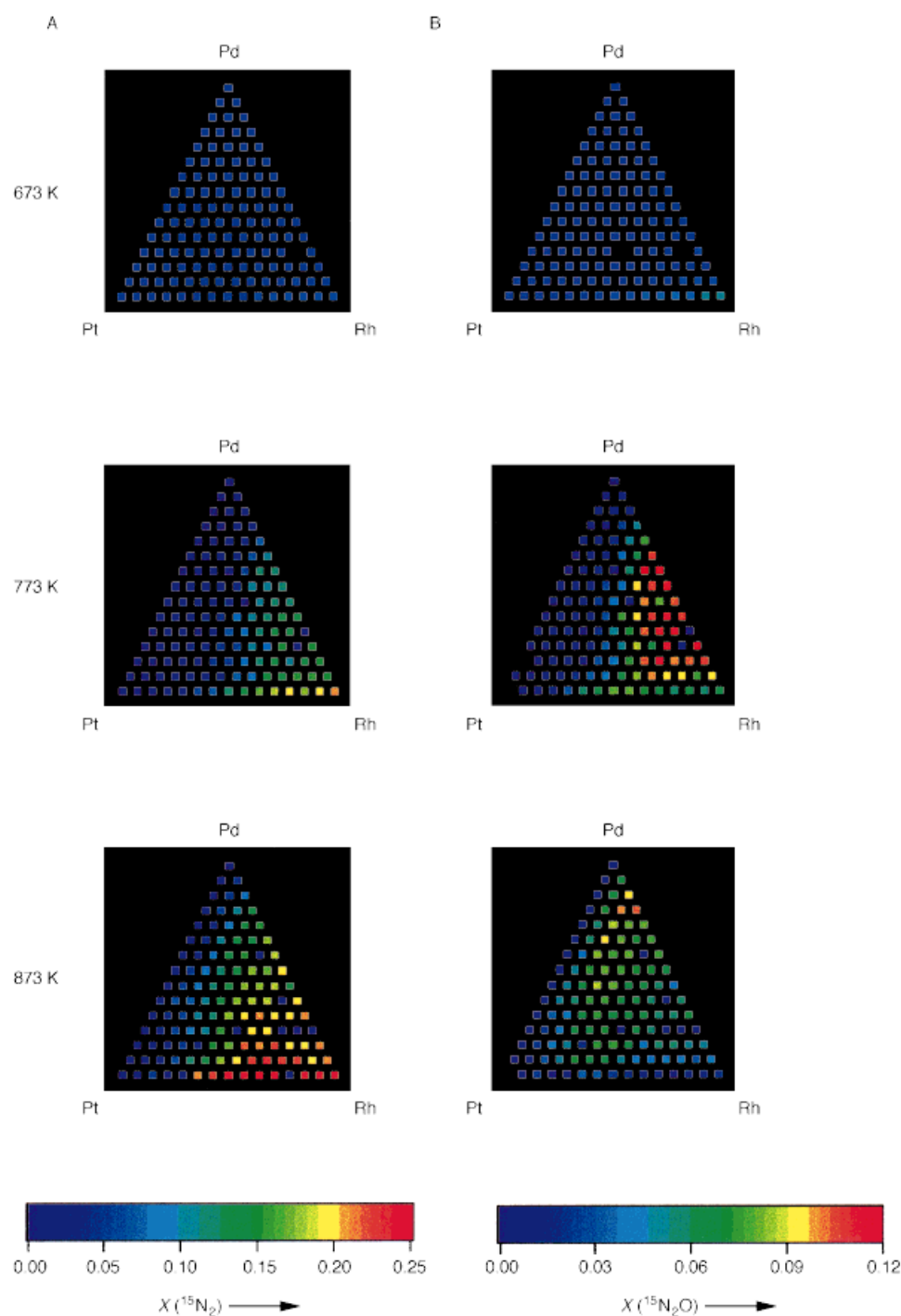


Figure 4. A) $^{15}\text{N}_2$ production (in units of 10^{-10} A ion current) from the same Rh-Pd-Pt library of Figure 2 at 673, 773, and 873 K. B) The corresponding $^{15}\text{N}_2\text{O}$ production from the same library. Note the different scales in the two cases.

- [6] E. Danielson, M. Devenney, D. M. Giaquinta, J. H. Golden, R. C. Haushalter, E. W. McFarland, D. M. Poojary, C. M. Reaves, W. H. Weinberg, X. D. Wu, *Science* **1998**, 279, 837–839.
- [7] F. C. Moates, M. Somani, J. Annamalai, J. T. Richardson, D. Luss, R. C. Wilson, *Ind. Eng. Chem. Res.* **1996**, 35, 4801–4803. A related patent application (PCT US 97/02756) is broader in scope, but of less interest since no experiments were run.
- [8] S. M. Senkan, *Nature* **1998**, 394, 350–352.
- [9] A. Holzwarth, H.-W. Schmidt, W. F. Maier, *Angew. Chem.* **1998**, 110, 2788–2792; *Angew. Chem. Int. Ed.* **1998**, 37, 2644–2647.
- [10] T. Engel, G. Ertl, *Adv. Catal.* **1979**, 28, 1–78.
- [11] K. C. Taylor, *Ind. Eng. Chem. Prod. Res. Dev.* **1976**, 15, 264–268.
- [12] R. M. Heck, R. J. Farrauto, *Catalytic Air Pollution Control: Commercial Technology*, Van Nostrand Reinhold, New York, **1995**.
- [13] The catalysts in the library were characterized by X-ray powder diffraction with a scanning microdiffractometer, GADDS from Bruker AXS. Data were measured with $\text{CuK}\alpha$ radiation (2-kW generator, $\lambda = 1.5418 \text{ \AA}$) in the range $10 < 2\theta < 72^\circ$ with an exposure time of 10 min per catalyst. The primary beam was focussed to a spot of 700 μm in diameter by means of bent Göbel mirrors and a collimator. The library was mounted on the XYZ stage of the diffractometer and initial alignments were carried out with a laser and video microscope assembly.
- [14] W. H. Weinberg, E. W. McFarland, P. Cong, S. Guan (Symyx Technologies), WO-A 98/15969 A2, **1998**.
- [15] J. A. Rodriguez, D. W. Goodman, *Surf. Sci. Rep.* **1991**, 14, 1–107.
- [16] J. Szanyi, D. W. Goodman, *J. Catal.* **1994**, 145, 508–515.

- [17] R. E. R. Colen, M. Kolodziejczyk, B. Delmon, J. H. Block, *Surf. Sci.* **1998**, 412, 447–457.
 [18] R. W. Vook, B. Oral, *Appl. Surf. Sci.* **1992**, 60, 681–687.
 [19] W. F. Egelhoff, Jr. in *The Chemical Physics of Solid Surfaces and Heterogeneous Catalysis*, Vol. 4 (Eds.: D. A. King, D. P. Woodruff), Elsevier, Amsterdam, **1982**, pp. 397–426.
 [20] K. C. Taylor, *Stud. Surf. Sci. Catal.* **1987**, 30, 97–116.
 [21] S. M. Vesecky, P. Chen, X. Xu, D. W. Goodman, *J. Vac. Sci. Technol. A* **1995**, 13, 1539–1543.

The Hume–Rothery Compound $\text{Mn}_8\text{Ga}_{27.4}\text{Zn}_{13.6}$: Separated Zn_{13} -Clusters Interspersed in a Primitive Cubic Host Lattice**

Ulrich Häussermann,* Per Viklund, Christer Svensson,
 Sten Eriksson, Pedro Berastegui, and Sven Lidin

The interpretation of structural stability and chemical bonding in intermetallic compounds is a continuous challenge in chemistry because metallic systems evade the simple and powerful rules developed by chemists which allow the linking of electron counts to particular geometrical arrangements of atoms.^[1, 2] However, there exists a number of intermetallic compounds where the valence electron concentration (VEC, average number of valence electrons per atom) plays a decisive role for structural stability, and these compounds are usually classified as electron compounds^[3] or Hume–Rothery compounds.^[4] One group of such Hume–Rothery compounds comprises E-rich systems T_mE_n ($n/m \geq 3$) where T is a transition metal from the V–Co groups and E is preferably Al or Ga. In these compounds the transition metal atoms appear uniformly distributed in a matrix of E atoms, and the resulting structures (e.g., VAl_{10} , WAl_{12} , MnAl_6 , Co_2Al_9 , MnGa_4 , V_8Ga_{41} , V_7Al_{45}) are very often large and complex. Remarkably the T atoms are separated by the largest distance possible and, thus, are only coordinated by E atoms in the first coordination sphere. The resulting TE_p coordination polyhedra are rather regular ($p = 8–12$) and appear as discrete

entities (VAl_{10} , WAl_{12}), as vertex-linked (Co_2Al_9 , MnGa_4 , V_8Ga_{41}), or as edge-linked (MnAl_6) networks. Many of these T_mE_n Hume–Rothery compounds were prepared and characterized 20 years ago, but have experienced a renaissance recently with the discovery of further examples such as MoAl_6 , WAl_6 , $\text{Mo}_5\text{Al}_{22}$, and the ternary $\text{Mo}_7\text{Sn}_{12}\text{Zn}_{40}$ by Hillebrecht et al.^[5]

The origin of the important role of VEC for the stability of this group of Hume–Rothery compounds lies in the occurrence of a pronounced pseudo gap in the density of states (DOS) which is a result of strong bonding between T and E atoms.^[6] We want to exemplify the characteristic features of the electronic structure of these compounds with the DOS of V_8Ga_{41} ^[7] shown in Figure 1 a: At low energy the density of

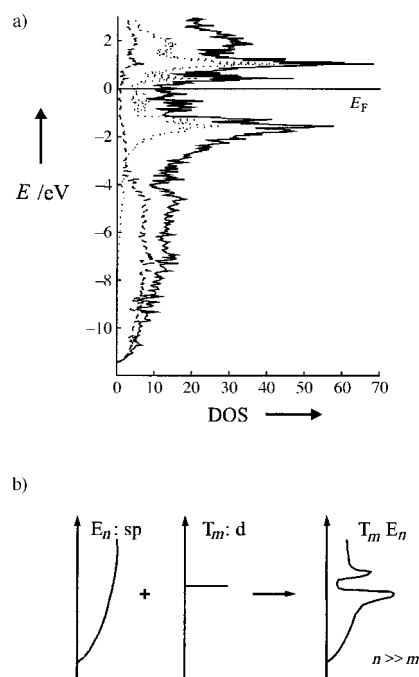


Figure 1. a) Total density of states (DOS (states/eV cell)) together with the d orbital contribution from V (dotted lines) and the s orbital contribution from Ga (dashed lines) of the compound V_8Ga_{41} as obtained from LMTO–ASA calculations. b) Schematic construction of the DOS of the T_mE_n Hume–Rothery compounds as a perturbation of free-electron like states of the E atom matrix by T atom d states.

states is dominated by approximately parabolically distributed (free-electron like) states stemming from the sp bands of the E atom matrix, which at higher energy are perturbed by the T atom d states. The strong d–sp interaction in these compounds opens up a pseudo gap (or sometimes even a narrow band gap) at or close to the Fermi level (E_F) which separates d–sp bonding and antibonding states. Figure 1 b summarizes in a simplified manner how the DOS of the T_mE_n Hume–Rothery compounds is built up by this perturbation process. As a consequence the TE_p coordination polyhedra represent strongly bonded entities, and the position of the pseudo gap determines the optimum VEC, or in the case of broad pseudo gaps a range of optimum VECs, for a particular Hume–Rothery compound. In V_8Ga_{41} ^[8] only one kind of TE_p polyhedron—corresponding to a VGa_{10} unit—occurs. This

[*] Dr. U. Häussermann, Prof. S. Lidin
 Department of Inorganic Chemistry, Stockholm University
 10691 Stockholm (Sweden)
 Fax: (+46)8-152187
 E-mail: ulrich@inorg.su.se
 Dr. P. Viklund, Dr. C. Svensson
 Department of Inorganic Chemistry 2
 Lund University (Sweden)
 S. Eriksson
 Studsvik Neutron Research Laboratory
 Uppsala University (Sweden)
 Dr. P. Berastegui
 ISIS Facility, Rutherford Appleton Laboratory
 Chilton, Didcot, Oxon (UK)

[**] This work was supported by the Swedish National Science Research Council (NFR) and the Göran Gustafsson Foundation.